Comparing different fatigue test methods at asphalt mastic level

Michael Steineder ⬤ · **Martin Johannes Peyer** · **Bernhard Hofko** ·
Mohit Chaudhary · **Nikhil Saboo** · **Ankit Gupta**

Abstract Latest research is focused on predicting the fatigue behavior of asphalt mixtures through cost-effective and simple test methods on asphalt mastic level (asphalt binder + mineral fines). There are numerous fatigue test methods for asphalt binders and mastic using the dynamic shear rheometer (DSR). However, up to now, the results of the different fatigue tests on DSR have not been directly compared. Therefore, four different asphalt mastic mixes were prepared, and each was tested with the two most popular fatigue tests [linear amplitude sweep (LAS) test and time sweep (TS) test] and then compared to each other. The TS tests were performed as stress-controlled and as strain-controlled tests. All LAS and TS tests were performed with cylindrical and hyperbolic specimen shapes to identify impact of specimen shape. Different fatigue criteria were applied for evaluation to investigate the comparability of the results. Stress-controlled TS tests, strain-controlled TS tests, and LAS tests reveal different rankings of fatigue performance. However, a dissipated energy approach can combine stress-controlled and strain-controlled TS tests into one fatigue curve. The hyperbolic specimen shape can be used for TS tests and results in the same rankings. The hyperbolic specimen shape is not applicable for LAS tests. A calculation model could be derived to establish a relationship between the measured and actual stresses and strains in the necking of a hyperbolic specimen. TS tests using the dissipated energy approach appear to be the most promising mastic fatigue tests.

Keywords DSR · Fatigue · Aspahlt mastic · Time sweep · LAS

M. Steineder (✉) · M. J. Peyer · B. Hofko
Institute of Transportation, Vienna University of
Technology, Karlsplatz 13/E230-3, 1040 Vienna, Austria
e-mail: michael.steineder@tuwien.ac.at

M. Chaudhary · N. Saboo · A. Gupta
Department of Civil Engineering, Indian Institute of
Technology (BHU), Varanasi, Uttar Pradesh 221005,
India

1 Introduction

The occurrence of cracks due to material fatigue, mainly caused by repeated traffic loads, is one of the most frequently encountered patterns of damage in asphalt pavements. The traffic-induced loads led to stresses and strains with each load cycle, which accumulated damage in the form of growing micro-cracks on the underside of the asphalt pavement which increased with duration. After these micro-cracks have combined to form macro-cracks, they would move up to the road pavement's surface. Therefore, the prevention of fatigue-related cracks plays a key role in sustainable asphalt pavement engineering [1, 2]. Numerous laboratory test methods for asphalt mixtures are reported in the literature to classify their

fatigue performance. Thus, the test equipment, specimen geometry, and loading configurations change for each test [1, 3]. Widely used test setups are the tension-compression test, the 2-point-bending beam test, the 3-point-bending beam test, the 4-point-bending beam test, and the indirect tensile test according to EN 12697-24 [4].

All of the above-mentioned tests have the same disadvantages: Specimen preparation and the testing are time-consuming and need high amounts of material and personpower. Besides, for each test setup, special test equipment is necessary. Therefore, there is a strong incentive to move the characterization of the fatigue performance from asphalt mixture level to the asphalt binder or mastic level.

A number of studies have already shown a connection between the fatigue behavior of asphalt mixtures and that of asphalt binder or asphalt mastic [5–8]. The test methods for asphalt binder or asphalt mastic for this purpose are primarily performed with DSR. However, different test setups are used. Therefore, the objective of this paper is to compare the most commonly used fatigue tests on DSR and examine the comparability, since no direct comparison has been made in any studies until now. This study forms part of a larger project to provide a reliable prediction of the fatigue performance of asphalt mixtures based on DSR fatigue tests on asphalt mastic. As a result of this study, those test setups and evaluation methods should be found to be comparable. Consequently, these fatigue tests can serve as a basis for a correlation with the fatigue performance on the asphalt mixture level.

1.1 Background

As a result of the Strategic Highway Research Program (SHRP), the Performance Grading (PG) specification according to AASHTO M 320-17 [9] was developed. Using a Dynamic Shear Rheometer (DSR), the viscoelastic properties of asphalt binders are evaluated in terms of the fatigue potential of asphalt mixes [10].

However, studies on this PG specification showed that the linear viscoelastic SHRP parameter used to evaluate fatigue performance ($|G^*|sin(\delta)$) did not correlate with the fatigue behavior of the respective asphalt mix, especially when modified asphalt binders are used [11].

As a further development, the Time-Sweep (TS) test was used to describe the fatigue behavior of asphalt binder. The basis for this test is the deterioration of material integrity under repeated loading. This loading model corresponds with the classical theory of pavement fatigue. The rolling wheel causes compressive and tensile stresses on the underside of an asphalt concrete layer due to the weight of the over rolling vehicle [12]. Due to a large number of vehicles, this creates a pulsating load, as applied in a TS test. In the TS test, sinusoidal loading at a defined frequency and stress or strain amplitude is used to test until material failure. However, there is no standardized criterion that defines fatigue failure for TS tests [13]. There are many different fatigue criteria in the literature. The most widely used criterion in the context of asphalt fatigue is the decrease in stiffness. It states that the specimen fails when the stiffness reaches 50% of the initial stiffness. It is defined in the AASHTO T 321 [14], EN12967-24 [4], and SHRP-A-404 [15].

A further definition of fatigue failure is the use of phenomenological parameters. For example, notable changes in damage progression such as the peak of the phase angle would define the failure of asphalt and mastic [16–18]. Dissipated energy approaches are also applicable as a definition of fatigue failure. These fatigue criteria comprise the dissipated energy ratio (DER) [6, 19–21] and the ratio of dissipated energy change (RDEC) [22–26]. Based on the dissipated energy approach, another simple phenomenological indicator was derived. The peak of the product value ($S \times N$), according to the multiplication of the stiffness ratio (S) and the load cycles (N), is used as a fatigue criterion [27]. The maximum SxN is also applied in ASTM D7460-10 for asphalt mixture [28].

The main advantage of TS tests is the simulation of a realistic loading. In addition, the parameters can be adjusted by controlling the temperature, frequency, and type of loading (stress- or strain-controlled). Furthermore, there is no restriction to the linear viscoelastic range. A significant disadvantage of this method is the long duration of the experiment (often several hours per experiment). In addition, the high stiffness of the mastics can bring the DSR to its performance limits. Motor cooling can also influence the results [29]. One way to minimize the system loading of the DSR is to use a hyperbolic specimen

shape. The hyperbolic specimen shape has a necking in the middle of the specimen [16]. This specimen shape reduces the necessary torque, which relieves the DSR. The disadvantage of the hyperbolic specimen shape is that the measured rheological data cannot be used without converting them. However, such a calculation model is currently not available. Nevertheless, the load cycles up to the fatigue criterion can be used to characterize the durability.

A quicker fatigue test on the DSR is the linear amplitude sweep (LAS) test. According to AASHTO TP101-14 [30], cylindrical asphalt binder samples with a diameter of 8 mm and a height of 2 mm are used as test specimens. The test procedure according to AASHTO TP101-14 [30] is divided into two sections. The first test section determines the material behavior and the rheological characteristics of the undamaged specimen through a strain-controlled frequency sweep test in the DSR. During the second test section, the specimen is subjected to a strain-controlled amplitude sweep test, performed at a constant frequency of 10 Hz and a constant test temperature. The amplitude of the applied shear strain is increased linearly from 0% to 30% throughout 3100 load cycles. By applying the viscoelastic continuum damage model (VECD) in the form of the associated formulas from AASTHO TP101 [30], a linear correlation can be found between the parameter load cycles and the expected shear strain in terms of a linear equation.

The main advantage of the LAS test is the very fast test procedure (approx. 20 min/test). In addition, by regulating the temperature, tests can be carried out at different temperature ranges. But, the results of LAS tests show only a low correlation with the results of other fatigue tests [11].

In addition to the tests mentioned above with the DSR, there are other test methods for determining the fatigue resistance of asphalt binder, such as the DENT [31] test method. However, as the DSR is a widely used laboratory instrument and is already part of the standard equipment of a road construction laboratory, only tests on the DSR were considered in this study.

1.2 Research approach

As part of a large study to accurately predict the fatigue behavior of asphalt mixtures based on fatigue testing of asphalt mastic, this work focuses on the applicability and comparability of the most popular

fatigue tests on DSR. Since asphalt mastic (asphalt binder + mineral fines) is the main binder component in asphalt mixes [32], fatigue tests are carried out at the mastic level in this study. On the one hand, mastic fills the spaces between the contact points of large aggregates, and on the other hand, mastic binds the aggregates together [33, 34]. The properties of asphalt mastic are primarily influenced by the relative amount of filler in relation to the asphalt binder content of the mix. Generally, the ratio of filler and asphalt binder used to produce the asphalt mastic is called filler - binder (F-B) ratio [35]. Studies by Liao et al. [2] using DSR on samples of asphalt mastic and asphalt binder have revealed changes in fatigue properties as a result of the addition of filler to asphalt binder. It was found that the stiffness of asphalt mastic, especially with increasing filler content, is significantly higher than that of pure asphalt binder. Furthermore, several studies [36–42] show that the physicochemical interaction between asphalt binder and fillers and the geometrical characteristics of the fillers impact the behavior of mastic.

This study compares the fatigue life of asphalt mastic resulting from different fatigue tests. The mode of loading, specimen geometries, and failure definitions vary. The clear objective of this study is to investigate the comparability of fatigue tests. On the one hand, the different modes of loading will be compared, and on the other hand, the different failure definitions will be compared. Due to the system limitations of DSR tests at higher material stiffness levels, comparability between cylindrical and hyperbolic specimens is also considered. The hyperbolic specimen shape allows the measurement of stiffer mastic samples. These results will then be used to screen out those test methods that will serve as the basis for a large-scale series of tests that will produce an accurate prediction model for the fatigue behavior of asphalt mixtures based on DSR fatigue testing of asphalt mastic. Since all tests are performed on two specimen shapes (cylindrical and hyperbolic), this study also attempts to derive a calculation apparatus that allows conversion of the measurement results between the two shapes. This study did not investigate the direct influences of different fillers (physio-chemical or geometric characteristics) on fatigue behavior.

2 Materials

For this study, we used four different fillers (predominantly grain size < 0.063 mm). Two fillers are from Europe, and two fillers are from India. The two European fillers are limestone and quartz. While limestone is a standard filler for asphalt mixes, quartz is an industrial product that is not used in road construction usually. Stone dust is also a standard filler for asphalt mixes, and glass powder is a by-product of the respective industries. Both fillers (quartz and glass powder) are mostly unexplored materials for asphalt mixes. However, based on the studies carried out so far, both materials show high potential for road construction. Due to the wide range of different materials, we expect a large spectrum of test results.

Asphalt mastic is a mixture of asphalt binder and mineral filler. For this study, a filler binder ratio of 1.5 by weight was selected. We used an asphalt binder with a penetration grading of 70/100 to mix the four different mastics. For the asphalt binder, the needle penetration depth (PEN) according to EN 1426 [43], the softening point (ring and ball) according to EN 1427 [44], and the performance grade (PG) according to AASHTO M 320 [9] was determined. The results are listed in Table 1.

For the preparation of the mastic samples, the two components, filler and asphalt binder, are weighed according to the filler-binder ratio. Next, the dry filler is heated to 180 °C in an oven for at least 1 h. Afterward, the asphalt binder is heated to 180 °C. Then the two materials are mixed manually for about 5 min, without heating, until the mixture starts to stiffen. The result is a homogeneous mastic, without fine particles can settle down to the bottom during cool down. Table 2 lists the mastic mixes produced with their source materials. The gravimetric filler binder ratio is the same for all mixes. However, due to the

Table 1 Properties of the asphalt binder used in this study

Properties	Values
Needle penetration depth (PEN) [1/10 mm]	85
Softening point (ring and ball) [°C]	45.4
Performance grade (PG)	64–28

different specific gravities, the filler volume ratio is not the same for all mixes, as shown in Table 2.

For the four mastic mixes and the plain asphalt binder, the softening point and the viscosity were determined. The viscosity was determined with a rotational viscometer for the temperature range from 120 to 180 °C. The results are summarized in Table 3. It can be seen that the addition of filler increases the viscosity and the softening point. While mastic 1 to 3 shows similar values, the mastic 4 with glass powder clearly exhibits the highest values. A correlation between filler-volume-ratio, softening point, and viscosity is discernible but not significant due to the small number of samples.

3 Test methods

The dynamic shear rheometer (DSR) is one of the essential instruments in a road engineering laboratory. Unlike other test equipment, it can be used for a variety of different test routines. Moreover, a large number of different parameters and properties can be derived from the rheological data. Therefore, it is evident that the fatigue behavior of asphalt should also be derived from simple tests at the mastic level. For this purpose, two test methods have asserted themselves in recent years. One is the time sweep (TS) test, and the other is the LAS test.

3.1 Fatigue tests with DSR

The LAS test is defined by AASHTO TP 101-14 [30]. This test method describes the determination of the fatigue resistance of asphalt binders against damage due to cyclic loading with linearly increasing load amplitudes. In this study, the test method is used for mastic samples. The LAS tests in this study are performed at a temperature of $+10$°C. Three replicates per mastic were performed for the LAS test.

The time sweep (TS) test is a well-proven and simple fatigue test. Similar to the loading situation in a road construction, a test specimen is subjected to cyclic loading until it fails. The load amplitude and frequency remain constant over time. However, no normative standardization is available for this test method. Accordingly, there are a large number of different test parameters mentioned in the literature. The temperature, the mode of loading, and the test

Table 2 Mixed mastic

Mixture	Binder	Filler	Filler-Binder Ratio [–]	Filler-volume Ratio [%]
Mastic 1 (M1)	70/100	Lime stone	1.5	24.2
Mastic 2 (M2)	70/100	Quartz	1.5	25.7
Mastic 3 (M3)	70/100	Stone dust	1.5	25.2
Mastic 4 (M4)	70/100	Glass powder	1.5	28.7

Table 3 Properties of the mixed mastics used in this study

	Asphalt Binder	Mastic 1	Mastic 2	Mastic 3	Mastic 4
Softening point [°C]	45.4	61.1	59.3	61.6	72.3
Viscosity at 120°C [mPas]	823	8038	9075	10394	41883
Viscosity at 135°C [mPas]	371	3625	3938	4429	16667
Viscosity at 150°C [mPas]	190	1908	1954	2267	7608
Viscosity at 165°C [mPas]	108	1108	1071	1288	3742
Viscosity at 180°C [mPas]	68	733	633	783	2008

frequency vary in particular. In this study, we perform all tests stress-controlled (CS) and strain-controlled (CD). All TS tests in this study are performed at a frequency of 30Hz. This frequency keeps the test duration as short as possible. A test temperature of $+10°C$ was chosen to avoid a too soft consistency due to a high-test temperature or a too-high stiffness due to too low-test temperature. For each TS test, nine individual tests are carried out at three different shear stresses or strains. For the stress-controlled tests, 300 kPa, 400 kPa, and 500 kPa for hyperbolic specimens and 700 kPa, 1000 kPa, and 1200 kPa for cylindrical specimens were selected stress levels. These stress levels were chosen to achieve similar load cycles to fatigue for both specimen shapes. However, due to the necking for hyperbolic specimens, this is a nominal stress for hyperbolic specimens, since the DSR calculates the stress for a cylindrical specimen and not the actual stress in the necking. For the strain-controlled tests, 0.5%, 0.75%, and 1.00% were chosen as the strain for both specimen geometries. A fatigue curve can be derived from the load cycles until fatigue and the selected loads. A variation of the frequency or temperature was not foreseen in this study due to the very high testing effort but will be further investigated within the research project.

3.2 Fatigue criterion of TS tests

The fatigue criterion is also not clearly defined for TS tests, so different fatigue criteria are considered in this study.

- **Reduction of stiffness (RS)** Reaching a stiffness modulus of 50% of the initial stiffness is a traditional fatigue criterion. It is widely used and is defined in the standard EN 12697-24 [4] for asphalt mix level.
- **Phase angle peak (PA)** The maximum phase angle is also used as a fatigue criterion. However, there is a slight difference between CS and CD tests. While in CS tests, an apparent rise with a definite maximum can be identified towards the end of the test, there is often a flat rise in CD tests, and there are often several high points.

The following approaches are based on dissipated energy. The energy approach for asphalt and asphalt binder was developed in 1972 by Van Dijk, Moreaud, Quedeville, and Uge. It states a relationship between the fatigue life (N_f) and the cumulative dissipated energy at failure [21, 45]. Energy is dissipated in mechanical work, heat generation, or damage during a load cycle for a viscoelastic material [20, 46].

- **Dissipated energy ratio (DER)** DER is one of the best-known dissipated energy approaches and is accepted among researchers as a fatigue criterion.

The dissipated energy is calculated for each load cycle (W_i) using equation 1.

$$W_i = \pi \cdot \sigma_i \cdot \gamma_i \cdot \sin(\delta_i) \tag{1}$$

W_i is the dissipated energy in cycle i, σ_i, is the stress level in cycle i, γ_i, is the strain level in cycle i, and δ_i is the phase angle in cycle i. The cumulative dissipated energy up to the loading cycle n is calculated by summing the dissipated energy of all loading cycles. Thus, the DER can be described as the ratio of the cumulative dissipated energy up to load cycle n and the dissipated energy in load cycle n, as shown in Eq. 2.

$$DER = \frac{\sum_{i=0}^{n} W_i}{W_n} \tag{2}$$

The DER increases linearly initially for both loading modes, CS and CD. However, with time, the DER deviates from the linear line. This deviation indicates fatigue. Bonnetti et al. [19] defined a parameter N_{p20} for the load cycles until fatigue. The parameter describes the number of load cycles until the DER deviates from the undamaged linear line by 20% [19]. This definition is used for both CD-TS and CS-TS tests in this study.

- **Ratio of dissipated energy change (RDEC)** The RDEC approach was proposed as a further development of fatigue characterization based on dissipated energy [23, 26]. The new criterion was defined as the change in dissipated energy between cycles n and $n + 1$ divided by the total dissipated energy until load cycle n. By dividing the result by the change of load cycles, the RDEC for each load cycle can be calculated. The approach of this new criterion is that a larger portion of the energy dissipates than in the cycle before when a material fails [24]. This behavior cannot be observed in the undamaged sample. The RDEC is defined as equation 3.

$$RDEC = \frac{W_{(n+1)} - W_n}{W_n \cdot ((n+1) - n)} \tag{3}$$

RDEC is the average ratio of the change in dissipated energy per load cycle in cycle n compared to cycle $n + 1$. Thus, W_n is the dissipated energy during load cycle n, and $W_{(n+1)}$ is the dissipated energy during load cycle $n + 1$. When

evaluating the RDEC, three phases can be observed: an initial phase of decreasing trend, a plateau phase, and a phase of rapid increase. For this study, a fatigue criterion for load cycles was chosen when the RDEC was twice as large as in the plateau phase. The plateau value is the mean value of all RDEC between decreasing and increasing trends.

3.3 Hyperbolic specimen shape

In addition, there are already different specimen shapes besides the cylindrical shape. So we ran all tests in this study with an alternative specimen geometry. A study [29] has shown that CS-TS tests with mastic specimens of high stiffness lead to unstable complex shear modulus changes. These changes affect the test result. The cooling of the DSR drive system could be the reason for this issue. Because of the high system load, a cooling of the drive system is necessary. Therefore, all tests were performed on hyperbolic specimens. The necking in the middle of the specimen reduces the system loading. So, the load on the drive system is much lower, and the cooling system's influence is minimized. Figure 1 shows the cylindrical profile on the left and the hyperbolic profile on the right.

However, this specimen shape has the problem that the recorded measurement data do not correspond to the actual measurement data. Due to the PP08 measurement geometry, the DSR calculates all data related to this diameter. However, the actual diameter in the necking is only 6mm. Therefore, a calculation model is needed to convert the recorded data to the actual diameter. Based on the generally applied formulas of the two-plate model for calculating the maximum shear stress and shear strain of viscous material, the following formulas were determined by comparing the two formulas of the respective specimen geometry with an additional conversion factor. For simplicity, a cylindrical specimen with 8mm diameter and 6mm diameter were compared. This procedure allows determining the magnitude of the conversion factor between the two specimen shapes. According to equations 4 to 8, a relationship could be established between the two measured values.

Fig. 1 Cylindric specimen shape (left) and hyperbolic specimen shape (right)

$$\frac{2 \cdot \text{Torque}_{\text{DSR}}}{\pi \cdot \text{Radius}_{\text{DSR,8mm}}^3} \cdot f_\tau = \frac{2 \cdot \text{Torque}_{\text{DSR}}}{\pi \cdot \text{Radius}_{\text{DSR,6mm}}^3} \tag{4}$$

$$f_\tau = \frac{\text{Radius}_{\text{DSR,8mm}}^3}{\text{Radius}_{\text{DSR,6mm}}^3} = \frac{8^3}{6^3} = 2{,}37 \tag{5}$$

$$\frac{\alpha_{\text{DSR,8mm}} \cdot \text{Radius}_{\text{DSR,8mm}}}{\text{High}_{\text{DSR,8mm}}} \cdot f_\gamma = \frac{\alpha_{\text{DSR,6mm}} \cdot \text{Radius}_{\text{DSR,6mm}}}{\text{High}_{\text{DSR,6mm}}} \tag{6}$$

$$f_\gamma = \frac{\text{Radius}_{\text{DSR,6mm}}}{\text{Radius}_{\text{DSR,8mm}}} = \frac{6}{8} = 0{,}75 \tag{7}$$

$$f_{G^*} = \frac{f_\tau}{f_\gamma} = \frac{2{,}37}{0{,}75} = 3{,}16 \tag{8}$$

To be able to validate this relationship, additional tests were carried out using a virtual test geometry. The virtual measurement geometry consists of a PP08 geometry, but the diameter was changed from 8mm to 6mm in the software. Thus, the data is calculated and recorded concerning the actual 6mm diameter. Based on these data, the theoretical approach according to formulas 4 to 8 can be checked. With the calculation factors from the formulas above, the measurement data could be converted in both directions. These measured data are, however, afflicted with several inaccuracies. For example, the hypothesis of a cylindrical specimen with a diameter of 6mm is not given since it is only a necking in the specimen. In addition, the set moment of inertia and the compliance correction are defined for a test geometry with 8mm and not for a 6mm diameter and could influence the calculations.

4 Results and discussion

Four different mastic mixes were tested in this study using two different test methods (LAS and TS) and two different specimen shapes (cylindric and hyperbolic). The TS tests were performed stress-controlled and strain-controlled. This test program results in 144 individual tests for the TS tests. For all 144 individual tests, the fatigue load cycles were evaluated based on the four fatigue criteria mentioned in the Sect. 3.2; Test Methods. A graphical illustration of the tests performed in this study can be found in Fig. 2.

4.1 Correlation of fatigue criterion

Table 4 summarizes the coefficient of determination of the linear regressions between the different fatigue load cycles for the tests with cylindrical specimen shapes. It can be seen that the calculated fatigue load cycles from different criteria correlate perfectly with each other for the TS-CS test. On the other hand, in the TS-CD test, the fatigue load cycles evaluated with the PA criteria do not correlate with the other evaluated load cycles. So, it can be assumed that the PA criterion is not suitable to describe the point of fatigue for mastic. This impracticality can also be observed in the measurement data. In TS-CD tests, the phase angle exhibits a different evolution over the test duration. No recurring trend can be detected in the phase angle curves.

Table 5 summarizes the coefficient of determination of the linear regressions between the fatigue load cycles from different criteria for the tests with hyperbolic specimen shapes. Again, it can be seen that the calculated load cycles for the TS-CS test correlate very well with each other. On the other hand, in the TS-CD test, only the fatigue load cycles evaluated with the RS criterion and the fatigue load
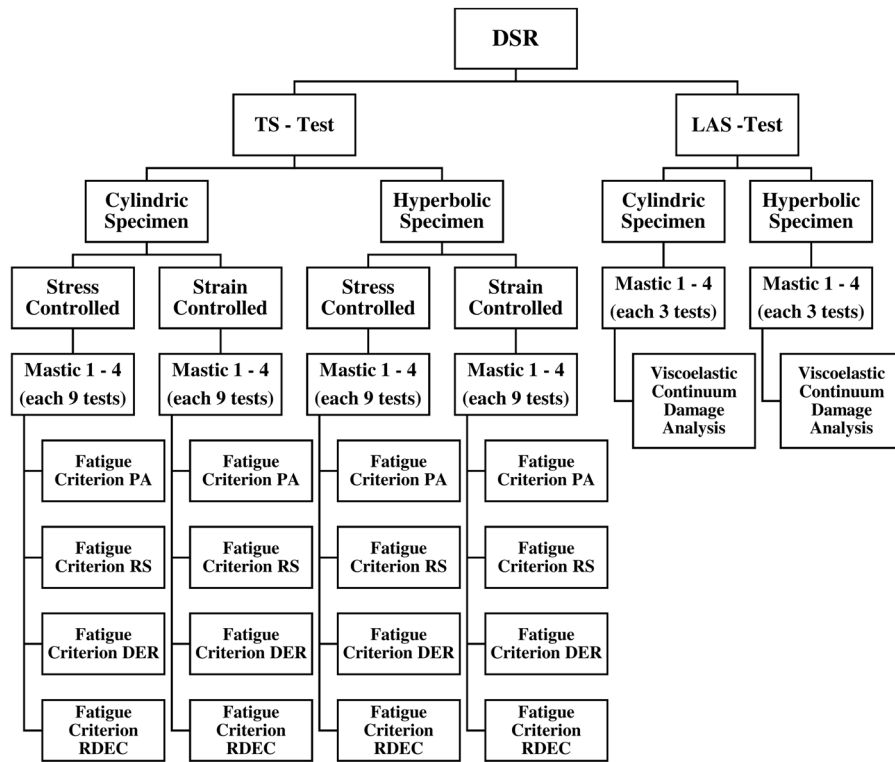
Fig. 2 Overview of the tests performed and the evaluation methods used

Table 4 Coefficient of determination of the linear regressions between the different fatigue load cycles for the tests with cylindrical specimen shape

	Stress controlled				Strain controlled			
	PA	RS	DER	RDEC	PA	RS	DER	RDEC
PA	1.000	1.000	0.999	0.999	1.000	0.450	0.453	0.425
RS		1.000	1.000	0.999		1.000	1.000	0.991
DER			1.000	0.999			1.000	0.992
RDEC				1.000				1.000

Table 5 Coefficient of determination of the linear regressions between the different fatigue load cycles for the tests with hyperbolic specimen shape

	Stress controlled				Strain controlled			
	PA	RS	DER	RDEC	PA	RS	DER	RDEC
PA	1.000	1.000	0.999	0.998	1.000	0.849	0.857	0.472
RS		1.000	0.999	0.998		1.000	0.998	0.507
DER			1.000	0.997			1.000	0.510
RDEC				1.000				1.000
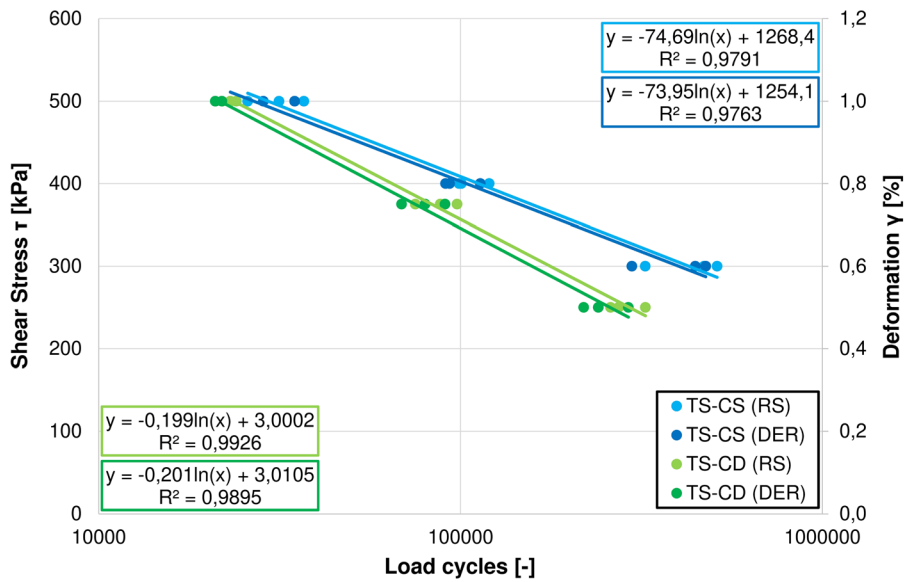
Fig. 3 Fatigue curves for the TS-CS and TS-CD tests on the hyperbolic specimen for mastic 2

cycles evaluated with the DER criterion correlate. Based on both evaluations, it can be concluded that for all four test methods (TS-CS and TS-CD with cylindrical specimen shape; TS-CS and TS-CD with hyperbolic specimen), the RS criterion and the DER criterion are suitable to define the point of fatigue. Both methods are already accepted fatigue criteria and can confirm each other. On average, the load cycles until fatigue using the DER criterion are about 7–10% smaller than using the RS criterion.

Due to the mentioned link between the fatigue criterion above, the RS criterion and the DER criterion will be used for the following evaluations.

4.2 Correlation of fatigue performance

According to the fatigue criteria, fatigue curves can be derived based on the load cycles. Fatigue curves are used to estimate the fatigue performance for different magnitudes of loading. This method is used in many areas of civil engineering. Based on the nine individual tests for each TS test, a fatigue curve can be derived. Figure 3 shows the fatigue curves for the TS-CS and TS-CD tests on the hyperbolic specimen for mastic 2. The two blue curves are the results of the TS-CS test with the different fatigue criteria. Correspondingly, the green curves represent the results of the TS-CD test with the different fatigue criteria.

To compare the results of the different fatigue tests, we calculated the required shear stress to achieve 10^5

Table 6 Required loads to achieve 10^5 load cycles for the different fatigue tests

Shape	Hyperbolic		Cylindric		Hyperbolic			Cylindric		
Test	TS - CS	TS - CS	TS - CS	TS - CS	TS - CD	TS - CD	LAS	TS - CD	TS - CD	LAS
Value	τ_5	τ_5	τ_5	τ_5	γ_5	γ_5	γ_5	γ_5	γ_5	γ_5
Crit.	RS	DER	RS	DER	RS	DER	–	RS	DER	–
Unit	[kPa]	[kPa]	[kPa]	[kPa]	[%]	[%]	[%]	[%]	[%]	[%]
Mastic 1	393.5	387.9	995.7	980.0	0.63	0.61	0.61	0.68	0.66	0.73
Mastic 2	410.1	404.2	1088.5	1075.9	0.72	0.69	0.67	0.76	0.74	0.85
Mastic 3	413.2	407.6	1049.2	1040.9	0.66	0.64	0.88	0.72	0.70	1.06
Mastic 4	468.0	459.9	1231.4	1212.7	0.61	0.59	0.60	0.66	0.64	1.14

load cycles for TS-CS tests. This shear stress is abbreviated as τ_5. For TS-CD tests, we calculated the required strain amplitude to achieve 10^5 load cycles. This strain value is abbreviated as γ_5. The same approach for TS-CD tests was also used for the LAS test. Thus, a γ_5 value can also be calculated for LAS tests.

Table 6 summarizes the loads required to achieve 10^5 load cycles for the different tests. It can be seen that the required loads for the DER criterion are about 1 to 3% smaller than the loads needed for the RS criterion to achieve 10^5 load cycles. Furthermore, it can be observed that the ranking of the mastic tests between hyperbolic specimens and cylindrical specimens is identical. This link cannot be observed in the LAS tests. Accordingly, it can be assumed that the LAS test is not directly applicable to hyperbolic specimen shapes. Furthermore, the ranking between TS-CS tests and TS-CD tests is not identical. For hyperbolic and cylindrical specimen shapes, a different order of the mastic mixture performances is obtained. As an example, we consider mastic 4. The TS-CS test displayed the best fatigue performance. For fatigue failure at 10^5 load cycles, it requires the highest shear stress of all 4 TS-CS tests. In the TS-CD tests, this is exactly the opposite. Here, the mastic 4 displayed the worst fatigue performance. It requires the smallest shear strain of all the TS-CD tests to reach 10^5 load cycles. As a result, it is not possible to directly compare the two different modes of loading. There is

also no correlation between the softening point or viscosity of the mastic and the fatigue performance. The main reason for the different rankings is expected to be affected by the modes of loading. In addition, in LAS tests, the high stiffness due to the low temperature and the use of mastic could affect the damage accumulation. The mode of loading is essential for selecting the test method and the interpretation of the results.

4.3 Dissipated energy approach

The fatigue tests performed in this study show that the mode of loading influences the assessment of the fatigue performance of the mastic mixes. However, the mode of loading should not be relevant when assessing fatigue performance. A method of linking TS-CS and TS-CD is via the dissipated energy approach. This approach allows combining the TS test results in one fatigue curve regardless of the mode of loading. One way to combine the two loading methods is the RDEC approach. The plateau value can be used to link the two loading methods. The disadvantage of this option is that the load cycles up to fatigue do not correlate well with the other fatigue methods. The reason for this is most likely the imprecise definition of the fatigue point and the range of the plateau value (start- and endpoint). There is no mathematical definition for this, so the analysis results are always dependent on the user to a certain extent.
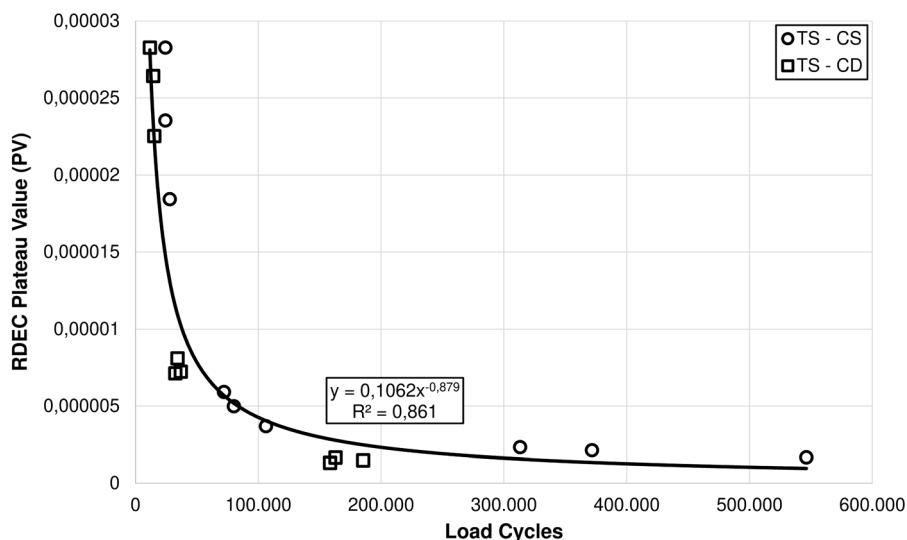

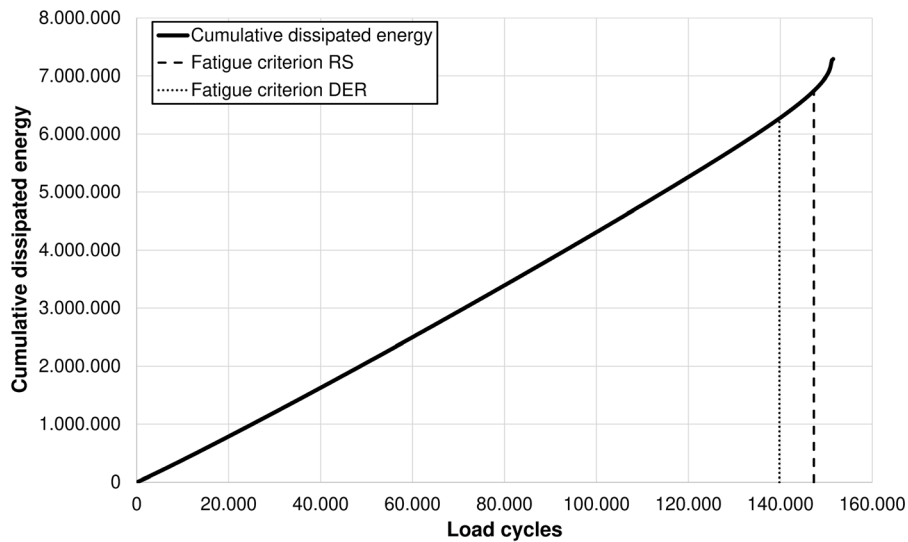**Fig. 4** Fatigue curve according to RDEC for mastic 1

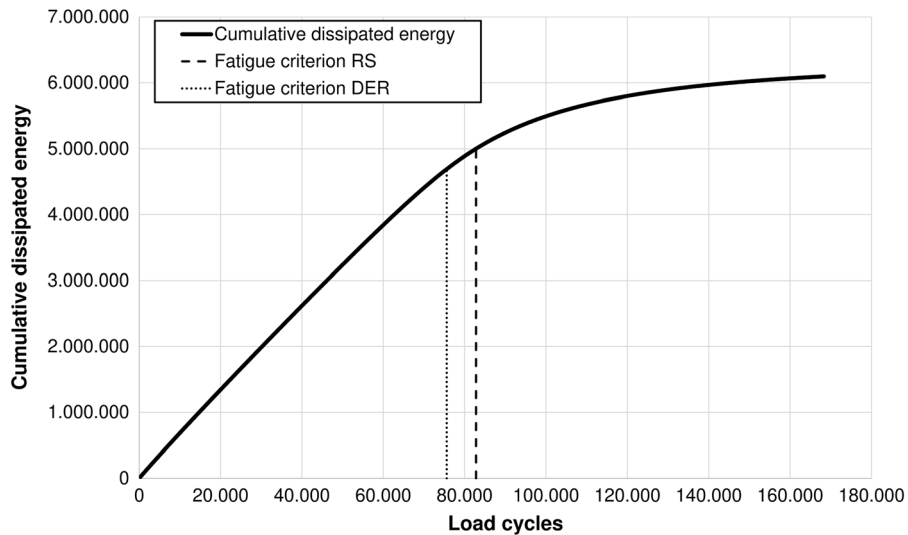**Fig. 5** Cumulative dissipated energy for a TS-CS test

Fig. 6 Cumulative dissipated energy for a TS-CD test

Figure 4 shows the fatigue curve according to RDEC for mastic 1. It shows that both loading methods can be combined. The coefficient of determination of the power-law regression is 0.861.

A new approach was used in this study to find a link between the TS-CS and TS-CD test for the fatigue criterion's RS and DER. Since the two fatigue criteria correlate perfectly, they were used for this approach. In Figs. 5 and 6, the cumulative dissipated energy for a TS-CS and a TS-CD test is depicted.

Figures 5 and 6 show that the curve of the dissipated energy is almost linear up to the two fatigue points. From this, it can be deduced that nearly the same energy is dissipated per load cycle. The initial input measurement parameter (stress or strain) can be brought to a uniform dimension (dissipated energy per load cycle). The dissipated energy per load cycle (DELC) calculation is given in equations 9 and 10.
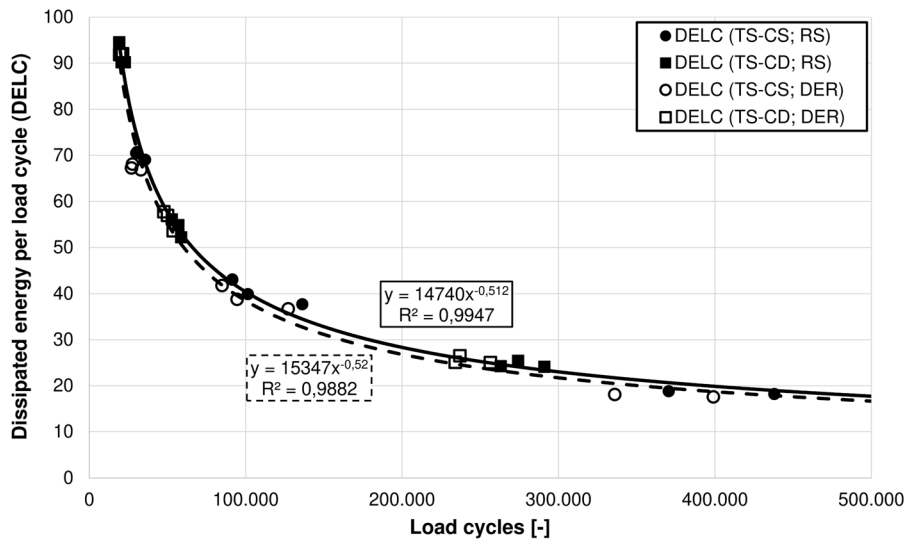
Fig. 7 DELC for the RS criterion and the DER criterion related to the load cycles for mastic 1 with cylindric specimen shape
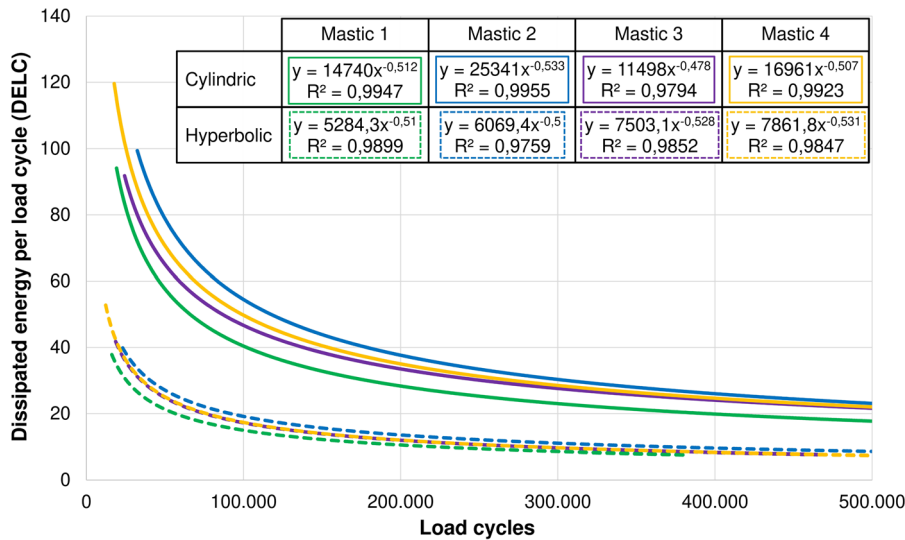
Fig. 8 Potency regression curves for all tests for cylindrical specimen shapes and hyperbolic specimen shapes

$$\text{DELC}_{\text{RS}} = \frac{\sum_{i=1}^{N_{\text{RS}}} Wi}{N_{\text{RS}}} \qquad (9)$$

$$\text{DELC}_{\text{DER}} = \frac{\sum_{i=1}^{N_{\text{DER}}} Wi}{N_{\text{DER}}} \qquad (10)$$

The results for TS-CS and TS-CD tests can be linked to one fatigue curve by using the above formulas. Figure 7 shows the DELC for the RS criterion and the DER criterion related to the load cycles for mastic 1 with cylindric specimen shape. The solid line is the power-law regression for the test evaluation using the RS criterion. The dashed line is the power-law regression for the test evaluation using the DER criterion. It can be seen that the DELC for the evaluations using the DER criterion is smaller than the DELC for the evaluations using the RS criterion. This difference coincides with all tests performed in this study. It can also be seen that a high fatigue load cycle number is achieved with a low DELC, whereas a

minimal fatigue load cycle number is achieved with a high DELC. With a coefficient of determination of 0.995 and 0.988, the regression is excellent.

Figure 8 shows the power-law regression curves for all tests for cylindrical specimen shapes and hyperbolic specimen shapes. The ranking of the mastic mixes remains the same for both specimen shapes. It can be seen that for cylindrical specimens, the DELC is higher than for hyperbolic specimen shape. Due to the higher load and the larger cross-sectional area of the specimen, more energy is dissipated. From Fig. 8, it can be deduced that the mastic that dissipates more energy per load cycle until failure perform better than the one with a smaller DELC value. This assertion means that mastic 2 has the best fatigue performance and mastic 1 the worst. The challange with this way of assessing the fatigue performance is that it is impossible to distinguish different effects of energy dissipation. Thus, the energy can be dissipated due to internal friction, viscous deformation, or fatigue. These energy dissipations and their proportions are influenced by the physicochemical interaction between asphalt binder and filler and the geometrical properties of the filler. These properties of the mastic are not part of this study, which is why no further analyses were carried out on this. However, due to the different fillers, it could be shown that the filler has a significant contribution to the fatigue performance of the mastic. Which properties of the filler affect the fatigue performance is the subject of current research.

Thus, there are a variety of ways to study the fatigue behavior of mastic. Since the TS test is not standardized, there are many different test methods and evaluation procedures. Comparing the data from Table 6 and Fig. 8, we see that the ranking of the results between hyperbolic and cylindrical specimen shapes does not show any differences. The regression coefficient of the linear correlation between cylindrical and hyperbolic specimen shape is higher than 0.98 for all TS tests. Only the LAS test shows no correlation between the two specimen shapes. On the other hand, the comparison between the different test methods shows partly different rankings of results. None of the tests (TS-CS, TS-CD, and LAS) is comparable with each other. The results also show that there is no correlation between the results ranking of RDEC and DELC. This observation means that the specimen shape does not influence the result in TS tests. Only the scale of the results changes according to the two specimen shapes. On the other hand, LAS tests with hyperbolic specimen shapes are not applicable without further adjustments in the calculation model of LAS. These adaptations are not part of this study.

4.4 Validation of calculation model for hyperbolic specimen shape

A theoretical relationship between cylindrical and hyperbolic specimen shape has already been established with equations 4 to 8. TS-CS tests were performed using a virtual 6mm test geometry. Since the virtual geometry causes the DSR to assume that it measures a cylindrical specimen with a diameter of 6mm, these values refer to the necking in the specimen shape. Thus, it can be checked whether the derived equations 4 to 8 can derive the approximate actual stresses and moduli based on the tests. Table 7 shows the measured values of Mastic 1 with an 8mm plate-plate test geometry (PP08) and a virtual 6mm plate-plate test geometry (VPP06).

According to equation 8, a factor between the complex shear modulus of 3.16 was calculated. Table 7 shows the mean value of the initial complex shear modulus of the mastic tests of mastic 1 using PP08 and VPP06. The factor between the measured results is 3.17. According to equations 4 and 5, a factor between the shear stresses of 2.37 was calculated. Table 7 summarizes the required shear stresses for 10^5 load cycles for PP08 and VPP06 for different fatigue criteria. The measured factor is 2.28 to 2.29, which is lower than the theoretical factor.

These slight deviations in the analyzed values are probably due to the simplifying assumption of a cylindrical specimen with a diameter of 6 mm. However, since this is a hyperbolic specimen shape, stress distribution in the necking is not identical to the stress distribution in a cylindrical specimen. In

Table 7 Correlation between the measured results with the PP08 and the VPP06

	PP08	VPP06	f [-]
$|G^*|_{\text{mean initial}}$ [Mpa]	84.63	267.95	3.17
τ_5 - PA [kPa]	396.66	908.77	2.29
τ_5 - RS [kPa]	393.53	900.65	2.29
τ_5 - DER [kPa]	387.91	884.15	2.28

addition, there are DSR specific correction values (compliance correction, moment of inertia of the test geometry), which have not been changed in the software. Only the diameter has been adjusted in the software from 8mm to 6mm. These settings could also influence the measurement results.

5 Conclusion

This study compares different fatigue test methods for asphalt mastic. There are various fatigue test methods available for asphalt binders performed with the DSR. These test methods were used in this study and examined at the mastic level. Four different mastic mixes were tested. Time sweep (TS) tests (stress and strain controlled) and LAS tests were performed. All tests were carried out on two different specimen shapes (cylindrical and hyperbolic). Different evaluation methods and fatigue criteria were used for the TS tests.

- In TS-CS tests, all fatigue criteria show a perfect correlation. The coefficient of determination of the linear regression of all fatigue load cycles is almost 1. In TS-CD tests, the fatigue criteria RS, DER, and RDEC correlate well with each other for cylindrical specimens. In TS-CD tests, the fatigue criteria RS and DER correlate well for hyperbolic specimens. Accordingly, it is recommended that the fatigue criteria RS or DER is used for TS tests.
- Considering the shear stress or shear strain required to achieve 10^5 load cycles, it can be observed that there is no correlation between the different fatigue tests. The fatigue performance of the mastics is ranked differently in each test method, due to the different modes of loading.
- A good approach to assessing fatigue performance is via dissipated energy. Through DELC or RDEC it is possible to combine stress and strain-controlled tests. Regardless of the loading mode in the test, uniform fatigue curves can be derived from the tests. The disadvantage of this method is that energy is dissipated not only by fatigue, but also by friction or viscous deformation. Therefore, it must still be determined whether the assessment using these values is possible, i.e. that energy dissipation is predominatly driven by fatigue. The classification of the mastics by DELC and RDEC show no correlation. One reason could be the user-dependent test evaluation of the RDEC method.
- A conversion of the measurement results between cylindrical and hyperbolic is confirmed. However. these are afflicted with inaccuracies. On the one hand, the derived equations are based on two cylindrical specimen shapes with different diameters. However, the stresses and strains in the necking of the hyperbolic specimen shape will differ slightly. On the other hand, the cylindrical specimen shape is influenced by trimming, which means that the same diameter of 8mm cannot always be guaranteed at all times.

The study shows that the results, due to different fatigue tests, do not all lead to the same classification of results. However, it is possible to combine stress- and strain-controlled tests using the dissipated energy approach. The fatigue criteria, especially the RS criterion and DER show a good applicability for all TS tests. The hyperbolic specimen shape is not applicable for LAS tests without adjustment. The LAS test may not be the ideal fatigue test for mastic with high stiffness due to low temperature or filler content because this affects the damage accumulation. However, TS tests using the dissipated energy approach appear to be the most promising mastic fatigue tests. Therefore, to identify the fatigue tests' classification, the tests at the mastic level should be compared with test series at the asphalt mix level. Influences due to different temperatures, frequencies and filler properties will be investigated in further studies. In addition, the effects on the test results of aged mastic specimens should be investigated since aged mastic samples have even higher stiffnesses.

Declarations

References

1. Di Benedetto H, De La Roche C, Baaj H, Pronk A, Lundstrom R (2004) Fatigue of bituminous mixtures. Mater Struct 37(3):202–216. https://doi.org/10.1007/BF02481620

2. Liao M-C, Chen J-S, Tsou K-W (2012) Fatigue characteristics of bitumen-filler mastics and asphalt mixtures. J Mater Civ Eng 24:916–923. https://doi.org/10.1061/(ASCE)MT.1943-5533.0000450

3. Poulikakos LD, Pittet M, Dumont A-G, Partl MN (2014) Comparison of the two point bending and four point bending test methods for aged asphalt concrete field samples. Mater Struct 48(9):2901–2913. https://doi.org/10.1617/s11527-014-0366-8

4. EN 12697-24 (2018) Bituminous mixtures-test methods—Part 24: resistance to fatigue. European Committee for Standardization (CEN), Brussels

5. Safaei F, Castorena C, Kim YR (2016) Linking asphalt binder fatigue to asphalt mixture fatigue performance using viscoelastic continuum damage modeling. Mech Time Depend Mater. https://doi.org/10.1007/s11043-016-9304-1

6. Johnson C, Bahia H, Coenen A (2009) Comparison of bitumen fatigue testing procedures measured in shear and correlations with four-point bending mixture fatigue. Paper presented at the 2nd conference on four point bending. University of Minho, Portugal

7. Steineder M, Donev V, Hofko B, Eberhardsteiner L (2021) Correlation between stiffness and fatigue behavior at asphalt mastic and asphalt mixture level. J Test Eval. https://doi.org/10.1520/JTE20210204

8. Soenen H, de La Roche C, Redelius P (2011) Fatigue behaviour of bituminous materials: from binders to mixes. Road Mater Pavement Des. https://doi.org/10.1080/14680629.2003.9689938

9. AASHTO M 320-17 (2017) Standard specification for performance-graded asphalt binder. American Association of State and Highway Transportation Officials (AASHTO), Washington, DC

10. Anderson DA, Kennedy TW (1993) Development of SHRP binder specification. Paper presented at the Asphalt Paving Technology Conference, Austin

11. Zhou F, Mogawer W, Li H, Andriescu A, Copeland A (2013) Evaluation of fatigue tests for characterizing asphalt binders. J Mater Civ Eng 25:610–617. https://doi.org/10.1061/(ASCE)MT.1943-5533.0000625

12. Raithby K, Sterling A (1972) Some effects of loading history on the fatigue performance of rolled asphalt. Transport Road Res Lab Rep 496:32

13. Wang C, Zhang H, Castorena C, Zhang J, Richard KY (2016) Identifying fatigue failure in asphalt binder time sweep tests. Construct Build Mater 121:535–546. https://doi.org/10.1016/j.conbuildmat.2016.06.020

14. AASHTO T 321 (2017) Standard Method of Test for Determining the Fatigue Life of Compacted Asphalt Mixtures Subjected to Repeated Flexural Bending. American Association of State and Highway Transportation Officials (AASHTO), Washington, DC

15. University of California, I. o. T. S. (1994) Fatigue response of asphalt-aggregate mixes. SHRP-A-404. Strategic Highway Research Program. National Research Council, Washington, DC

16. Hospodka M, Hofko B, Blab R (2018) Introducing a new specimen shape to assess the fatigue performance of asphalt mastic by dynamic shear rheometer testing. Mater Struct. https://doi.org/10.1617/s11527-018-1171-6

17. Kim Y-R, Little DN, Lytton RL (2003) Fatigue and healing characterization of asphalt mixtures. J Mater Civ Eng 15(1):75–83. https://doi.org/10.1061/(asce)0899-1561(2003)15:1(75)

18. Reese R (1997) Properties of aged asphalt binder related to asphalt concrete fatigue life. Paper presented at the Asphalt Paving Technology Conference, Salt Lake City

19. Bonnetti KS, Nam K, Bahia HU (2002) Measuring and defining fatigue behavior of asphalt binders. Bituminous Binders 2002(1810):33–43

20. Rowe G (1993) Performance of asphalt mixtures in the trapezoidal fatigue test. J Assoc Asphalt Paving Technol 62:344–384

21. Van Dijk W & Visser W (1977) Energy approach to fatigue for pavement design. Paper presented at the Technical Session of the Association of Asphalt Paving Technologists Proc, San Antonio

22. Boudabbous M, Millien A, Petit C, Neji J (2013) Shear test to evaluate the fatigue of asphalt materials. Road Mater Pavement Des 14(sup1):86–104. https://doi.org/10.1080/14680629.2013.774748

23. Carpenter S, Shen S (2006) Dissipated energy approach to study hot-mix asphalt healing in fatigue. Transp Res Rec J Transp Res Board 1970:178–185. https://doi.org/10.1177/0361198106197000119

24. Ghuzlan KA, Carpenter SH (2000) Energy-derived, damage-based failure criterion for fatigue testing. Transp Res Rec J Transp Res Board 1723(1):141–149. https://doi.org/10.3141/1723-18

25. Shen S, Carpenter S (2005) Application of the dissipated energy concept in fatigue endurance limit testing. Transp Res Rec 1929:165–173. https://doi.org/10.3141/1929-20

26. Shen SH, Airey GA, Carpenter SH, Huang H (2006) A dissipated energy approach to fatigue evaluation. Road

Mater Pavement Des 7(1):47–69. https://doi.org/10.3166/Rmpd.7.47-69

27. Rowe G, Bouldin MG (2000) Improved techniques to evaluate the fatigue resistance of asphaltic mixtures (2000). In: Proceedings of the papers submitted for review at 2nd Eurasphalt and Eurobitume Congress, Barcelona, Spain (2000)

28. ASTM D7460-10 (2019) Standard test method for determining fatigue failure of compacted asphalt concrete subjected to repeated flexural bending. ASTM International, West Conshohocken

29. Kim YS, Sigwarth T, Büchner J, Wistuba MP (2021) Accelerated dynamic shear rheometer fatigue test for investigating asphalt mastic. Road Mater Pavement Des 22(sup1):383-S396. https://doi.org/10.1080/14680629.2021.1911832

30. AASHTO TP 101-14 (2012) Standard method of test for estimating fatigue resistance of asphalt binders using the linear amplitude sweep. American Association of State and Highway Transportation Officials (AASHTO), Washington, DC

31. MTO LS-299 (2001) Method of test for the determination of asphalt cement's resistance to ductile failure using double edge notched tension test (DENT). Ministry of Transportation, Ontario

32. Grabowski W, Wilanowicz J (2007) The structure of mineral fillers and their stiffening properties in filler-bitumen mastics. Mater Struct. https://doi.org/10.1617/s11527-007-9283-4

33. Chen J-S, Peng C-H (1998) Analyses of tensile failure properties of asphalt-mineral filler mastics. J Mater Civ Eng. https://doi.org/10.1061/(asce)0899-1561(1998)10:4(256)

34. Recasens RM, Martinez A, Jimenez FP, Bianchetto H (2005) Effect of filler on the aging potential of asphalt mixtures. Transp Res Rec J Transp Res Board. https://doi.org/10.1177/0361198105190100102

35. Chaudhary M, Saboo N, Gupta A, Hofko B, Steineder M (2020) Assessing the effect of fillers on lve properties of asphalt mastics at intermediate temperatures. Mater Struct. https://doi.org/10.1617/s11527-020-01532-6

36. Huang SC, Zeng M (2007) Characterization of aging effect on rheological properties of asphalt-filler systems. Int J Pavement Eng. https://doi.org/10.1080/10298430601135477

37. Anderson D, Goetz W (1973) Mechanical behavior and reinforcement of mineral filler-asphalt mixtures. Joint Highway Research Project, Indiana Department of Transportation and Purdue University, West Lafayette, Indiana. FHWA/IN/JHRP-73/05. https://doi.org/10.5703/1288284313845

38. Pereira L et al (2018) Experimental study of the effect of filler on the ductility of filler-bitumen mastics. Construct Build Mater. https://doi.org/10.1016/j.conbuildmat.2018.09.063

39. Tunnicliff D (1962) A review of mineral filler. In: Proceedings of Association of Asphalt Paving Technologists, vol 31

40. Kallas B, Puzinauskas V, Krieger H (1961) A study of mineral fillers in asphalt paving mixtures. In: Proceedings of Association of Asphalt Paving Technologists, vol 30

41. Antunes V, Freire A, Quaresma L, Micaelo R (2015) Influence of the geometrical and physical properties of filler in the filler–bitumen interaction. Construct Build Mater. https://doi.org/10.1016/j.conbuildmat.2014.12.008

42. Clopotel C, Velasquez R, Bahia H (2012) Measuring physico–chemical interaction in mastics using glass transition. Road Mater Pavement Des. https://doi.org/10.1080/14680629.2012.657095

43. EN 1426 (2015) Bitumen and bituminous binders—determination of needle penetration. European Committee for Standardization (CEN), Brussels

44. EN 1427 (2015) Bitumen and bituminous binders—determination of the softening point—ring and ball method. European Committee for Standardization (CEN), Brussels

45. Van Dijk W, Moreaud H, Quedeville A, Uge P (1972) The fatigue of bitumen and bituminous mixes. In: Paper presented at the third international conference on the structural design of asphalt pavements, Grosvenor House, London

46. Rowe G (1996) Application of the dissipated energy concept to fatigue cracking in asphalt pavements. Thesis submitted to the University of Nottingham for the degree of Doctor of Philosophy